Progress In Electromagnetics Research, PIER 34, 143–163, 2001

FAST AND EFFICIENT ANALYSIS OF INSET DIELECTRIC GUIDE USING FOURIER TRANSFORM TECHNIQUE WITH A MODIFIED PERFECTLY MATCHED BOUNDARY

H. Jia

Department of Electrical and Electronic Engineering
Nagasaki University
Nagasaki 852-8521, Japan

K. Yasumoto and K. Yoshitomi

Department of Computer Science and Communication Engineering
Kyushu University
36, Fukuoka 812-8581, Japan

Abstract—A fast and efficient method for analyzing an inset dielectric guide is presented using the Fourier transform technique with a modified perfectly matched boundary. In order to deal with an open region, a novel idea, modified perfectly matched boundary condition (PMB), has been proposed. By introducing the modified PMB, the numerical integral has been avoided and the accuracy of the numerical solution has been improved. Moreover, the singular behavior of the fields at metal edge is taken into account in the analysis. The numerical examples are shown that the convergence of the solution is very fast and the relative error less than 0.07% is attained even if only the first term is considered in the field expansion of the guide. The numerical results of the propagation constants for single- and double-layered inset dielectric guides agree well with those of literatures.

Appendix A. Proof of the Modified PMB Condition

References

1. INTRODUCTION

An inset dielectric guide consisting of a rectangular groove filled with a dielectric medium is a low-loss transmission line in microwave and millimeter wave range [1–4]. Due to the low-cost and easy fabrication, the inset dielectric guide is expected as a promising devise for millimeter-wave integrated circuits and surface wave antennas with a low cross-polarization [5, 6]. During the past decade, the modal properties of the guide are extensively investigated by using the effective dielectric constant method [7], the transverse resonance diffraction method [6, 8–10], and mode matching method [11]. The effective dielectric constant method utilizes the transverse resonance condition for an equivalent structure with an effective dielectric constant. The transverse resonance diffraction method derives an integral equation for the aperture field of the groove, which is solved by using the Galerkin's method taking into account the field singularity at the metal edge. In the mode-matching method, the parallel metal walls is assumed at some distance away from the groove in the lateral direction and the fields in the cover region are approximated in terms of discrete parallel-plate waveguide modes.

In this paper, we propose an efficient method for analyzing an inset dielectric guide using the Fourier transform technique combined with a modified perfectly matched boundary(PMB). In this approach, the semi-infinite region over the guide is divided into two sub-regions, and a virtual boundary of perfectly electric conductor (PEC) or perfectly magnetic conductor (PMC) is assumed in the upper sub-region. Under the assumed boundary, the fields in each sub-region are represented by the Fourier integral and matched to those inside the guide expressed in terms of normal modes. Since the original semi-infinite region is replaced by the bounded region, and this mode-matching procedure is performed using a simple residual calculus, then an infinite set of linear equations is obtained. In order to obtain a fast convergence of the solution, the tangential components of the electric fields on the aperture are expanded in terms of the Gegenbauer polynomials multiplied by weighted functions [2], which satisfy the field singularity at the metal edge. This enables us to transform the original set of linear equations into a new set of equations with very fast convergence. Moreover since the components of electric field is independently expanded, this method is easily applied to complex

edges. It is shown that the convergence of our numerical results is very fast and the relative error is one quarter or less of those obtained by the transverse resonance diffraction method [2] under the same condition. The numerical results for single- and double-layered inset dielectric guides agree well with those of literatures [2, 8, 10]

2. MODIFIED PERFECTLY MATCHED BOUNDARY CONDITION

When open-waveguide structures are concerned, we experience inevitably a common troublesome related to the fields representation in the open region. The fields in the open region are expressed in terms of the continuous Fourier spectrum. This requires a numerical integration in spectral domain to obtain the solutions. One possible way to avoid such a numerical integration is to assume a fictitious PEC or PMC boundary at a fixed distance away from the open-waveguide. In this paper, we propose a novel idea for the perfectly matched boundary to deal with the open region. The similar idea has been proposed by Shen and Macphie [12] for analyzing a monopole antenna fed by coaxial lines. However their PMB model is not suitable for the eigenvalue problems of open-waveguides. To apply the idea of PMB to the eigenvalue problems, we shall propose a modified PMB by introducing a buffer region, in which the fields satisfying PEC couple with those of PMC fields under a prescribed condition. The boundary conditions of the fields of modified PMB can be written on the boundary $y = y_a$ of the buffer layer as follows:

$$\frac{E_{xe,ze}(x, y_a, z) + E_{xm,zm}(x, y_a, z)}{2} = E^{\mathrm{I}}_{x,z}(x, y_a, z) \qquad (1)$$

$$\frac{H_{xe,ze}(x, y_a, z) + H_{xm,zm}(x, y_a, z)}{2} = H^{\mathrm{I}}_{x,z}(x, y_a, z) \qquad (2)$$

with the additional constraints which are given by any two of four equations as

$$E_{xe,ze}(x, y_a, z) = E_{xm,zm}(x, y_a, z) \qquad (3)$$

$$H_{xe,ze}(x, y_a, z) = H_{xm,zm}(x, y_a, z). \qquad (4)$$

Note that two equations chosen from (3) and (4) are necessary to determine the fields uniquely, because the left hand sides of (1) and (2) contain four unknowns and the right hand sides contain two unknowns. It is noted that the sum of the reflected fields from the PEC and PMC walls becomes zero for any frequency and any polarization, when the

incident fields are same for the both walls located at the same position. These conditions are expressed by the following four equations:

$$E^+_{xe,ze}(x, y_a, z) = E^+_{xm,zm}(x, y_a, z) \quad (5)$$

$$H^+_{xe,ze}(x, y_a, z) = H^+_{xm,zm}(x, y_a, z). \quad (6)$$

The superscript + denotes the fields propagating in the plus y-direction with the y dependence of $e^{-j\eta y}$, where Im $(\eta) \leq 0$. If the equations (5) and (6) were applied instead of (3) and (4) as the additional constraints, we can obtain an ideal PMB which yields the fields exactly same as those of the original open-structure without PEC and PMC. However the process of such exact formulation reduces the problem again to the original one including the continuous spectrum. On the other hand, we note that the guided waves are evanescent in the y-direction in the open region, i.e., the amplitudes of the reflected waves $(\boldsymbol{E}^-, \boldsymbol{H}^-)$ from the PEC or PMC boundary are much less than those of the corresponding incident waves $(\boldsymbol{E}^+, \boldsymbol{H}^+)$. Then the incident fields given by (5) and (6) are well approximated by the total fields $(\boldsymbol{E}^+ + \boldsymbol{E}^-, \boldsymbol{H}^+ + \boldsymbol{H}^-)$ which are defined by (3) and (4). The detail proof is shown in the Appendix. The introduction of this approximation leads to the modified PMB. It is shown that the solutions obtained by the modified PMB converge very fast and the accuracy is superior to the conventional PEC boundary or PMC boundary.

3. FORMULATION

The cross section of an inset dielectric guide is shown in Figure 1, where a boundary of perfectly electric conductor or perfectly magnetic conductor is a virtual boundary introduced for the convenience of analysis. The cross sectional area is divided into three regions I, II, and III′. The strip region II is an additional buffer to improve calculating accuracy. The region III′ is the upper semi-infinite $(y > d)$ free-space of the original guide without PEC and PMC boundaries, and the region III denotes the free-space within $d \leq y \leq c$ bounded by the virtual PEC and PMC boundaries. The electromagnetic fields in the region I are derived from the electric and magnetic Hertzian vectors expressed as

$$\boldsymbol{\Pi}^h_{\mathrm{I}}(x, y, z) = \frac{\hat{y}e^{-j\beta z}}{k_1 k_0 Z_0} \sum_{m=0}^{\infty} A^h_m \frac{\sin\alpha_m(y+b)}{\sin(\alpha_m b)} \cos\tau_m(x+a) \quad (7)$$

$$\boldsymbol{\Pi}^e_{\mathrm{I}}(x, y, z) = \frac{\hat{y}e^{-j\beta z}}{k_1^2} \sum_{m=1}^{\infty} A^e_m \frac{\cos\alpha_m(y+b)}{\sin(\alpha_m b)} \sin\tau_m(x+a) \quad (8)$$

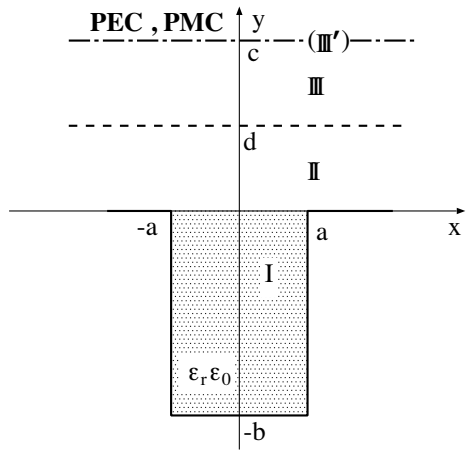

Figure 1. Cross section of a single-layered inset dielectric waveguide with a virtual boundary.

where $k_0 = \omega\sqrt{\epsilon_0\mu_0}$, $k_1 = k_0\sqrt{\epsilon_r}$, $\tau_m = \frac{m\pi}{2a}$, $\alpha_m = \sqrt{k_1^2 - \beta^2 - \tau_m^2}$, $Z_0 = \sqrt{\mu_0/\epsilon_0}$ is the intrinsic impedance in free space, β is the propagation constant of the guided mode, and A_m^h and A_m^e are unknown coefficients. We note that the electric field denoted by eqns. (7) and (8) satisfies the boundary conditions on the walls at $x = \pm a$, and $y = -b$. The fields in the region Ⅱ can be expressed by the Fourier integrals as follows:

$$\mathbf{\Pi}_{\mathrm{II}}^h(x,y,z) = \frac{\hat{y}}{k_0^2 Z_0}\frac{1}{2\pi}\int_{-\infty}^{\infty} e^{-j(\xi x+\beta z)}\Big[A^h(\xi)\sin\eta(y-d)+B^h(\xi)\sin(\eta y)\Big]d\xi \tag{9}$$

$$\mathbf{\Pi}_{\mathrm{II}}^e(x,y,z) = \frac{\hat{y}}{k_0^2}\frac{1}{2\pi}\int_{-\infty}^{\infty} e^{-j(\xi x+\beta z)}[A^e(\xi)\cos\eta(y-d)+B^e(\xi)\cos(\eta y)]\,d\xi \tag{10}$$

where $\eta = \sqrt{k_0^2 - \beta^2 - \xi^2}$, $A^h(\xi)$ to $B^e(\xi)$ are unknown spectral functions, and an infinitesimal small loss has been assumed in the wavenumber k_0 of free space, which is finally reduced to zero. The field components in the region Ⅲ are derived from the Hertzian vectors expressed by Fourier integrals as

$$\mathbf{\Pi}_{\mathrm{III}e}^h(x,y,z) = \frac{\hat{y}}{k_0^2 Z_0}\frac{1}{2\pi}\int_{-\infty}^{\infty} C^h(\xi)\sin\eta(y-c)e^{-j(\xi x+\beta z)}d\xi \tag{11}$$

$$\mathbf{\Pi}^{e}_{\text{III}e}(x,y,z) = \frac{\hat{y}}{k_0^2}\frac{1}{2\pi}\int_{-\infty}^{\infty} C^{e}(\xi)\cos\eta(y-c)e^{-j(\xi x+\beta z)}d\xi \quad (12)$$

$$\mathbf{\Pi}^{h}_{\text{III}m}(x,y,z) = \frac{\hat{y}}{k_0^2 Z_0}\frac{1}{2\pi}\int_{-\infty}^{\infty} D^{h}(\xi)\cos\eta(y-c)e^{-j(\xi x+\beta z)}d\xi \quad (13)$$

$$\mathbf{\Pi}^{e}_{\text{III}m}(x,y,z) = \frac{\hat{y}}{k_0^2}\frac{1}{2\pi}\int_{-\infty}^{\infty} D^{e}(\xi)\sin\eta(y-c)e^{-j(\xi x+\beta z)}d\xi \quad (14)$$

where $\eta = \sqrt{k_0^2-\beta^2-\xi^2}$ and $C^h(\xi)$ to $D^e(\xi)$ are unknown spectral functions. The fields $(\boldsymbol{E}_{\text{III}e}, \boldsymbol{H}_{\text{III}e})$ satisfy the PEC boundary conditions at $y = c$, and the fields $(\boldsymbol{E}_{\text{III}m}, \boldsymbol{H}_{\text{III}m})$ satisfy the PMC boundary conditions at $y = c$. The tangential components of electric and magnetic fields derived from (7)–(14) should be continuous across the boundaries $y = 0$, and the fields on the plane $y = d$ satisfy the modified PMB condition as described in (1)–(4), here we choose equation (3) to be the additional constraint equations.

$$E^{\text{II}}_{x,z}(x,0,z) = \begin{cases} E^{\text{I}}_{x,z}(x,0,z) & |x|<a \\ 0 & \text{otherwise} \end{cases} \quad (15)$$

$$H^{\text{II}}_{x,z}(x,0,z) = H^{\text{I}}_{x,z}(x,0,z) \qquad |x|<a \quad (16)$$

$$E^{\text{III}e}_{x,z}(x,d,z) = E^{\text{III}m}_{x,z}(x,d,z) = E^{\text{II}}_{x,z}(x,d,z) \quad (17)$$

$$2H^{\text{II}}_{x,z}(x,d,z) = H^{\text{III}e}_{x,z}(x,d,z) + H^{\text{III}m}_{x,z}(x,d,z) \quad (18)$$

The boundary condition for the electric fields at $y = d$ are first applied. The electric fields derived from (9)–(14) are substituted into (17), and Fourier transforms are calculated, then we obtain

$$\begin{cases} C^{e}(\xi) = \dfrac{\sin(\eta d)}{\sin\eta(d-c)}B^{e}(\xi) \\ C^{h}(\xi) = \dfrac{\sin(\eta d)}{\sin\eta(d-c)}B^{h}(\xi) \end{cases} \quad (19)$$

$$\begin{cases} D^{e}(\xi) = -\dfrac{\sin(\eta d)}{\cos\eta(d-c)}B^{e}(\xi) \\ D^{h}(\xi) = \dfrac{\sin(\eta d)}{\cos\eta(d-c)}B^{h}(\xi). \end{cases} \quad (20)$$

Using (19) and (20) into (11)–(14), the magnetic fields on the plane $y = d$ can be derived from (9)–(14) that contain only the unknown functions of $B^e(\xi)$ and $B^h(\xi)$. Substituting these results into the relationship (18), and taking Fourier transform with respect to x, then we have

$$B^{h}(\xi) = \Theta A^{h}(\xi), \qquad B^{e}(\xi) = \Theta A^{e}(\xi) \quad (21)$$

where $\Theta = \sin 2\eta(d-c)/\sin\eta(2c-d)$. From (7) and (8) the tangential components of the electric fields on the aperture can be derived as follows:

$$E_z^{\mathrm{I}}(x,0,z) = j\sum_{m=0}^{\infty}\left[\frac{\tau_m}{k_1}A_m^h + \frac{\beta\alpha_m}{k_1^2}A_m^e\right]\sin\tau_m(x+a)e^{-j\beta z} \quad (22)$$

$$E_x^{\mathrm{I}}(x,0,z) = \sum_{m=0}^{\infty}\left[\frac{\beta}{k_1}A_m^h - \frac{\tau_m\alpha_m}{k_1^2}A_m^e\right]\cos\tau_m(x+a)e^{-j\beta z}. \quad (23)$$

In the same way, the electric fields in the region Ⅱ can be derived from (9) and (10).

$$E_z^{\mathrm{II}}(x,0,z) = -\frac{1}{2\pi}\int_{-\infty}^{\infty}\left[\frac{j\eta\beta}{k_0^2}A^e(\xi) - \frac{\xi}{k_0}A^h(\xi)\right]\sin(\eta d)e^{j(\xi x+\beta z)}d\xi \quad (24)$$

$$E_x^{\mathrm{II}}(x,0,z) = -\frac{1}{2\pi}\int_{-\infty}^{\infty}\left[\frac{j\xi\eta}{k_0^2}A^e(\xi) + \frac{\beta}{k_0}A^h(\xi)\right]\sin(\eta d)e^{-j(\xi x+\beta z)}d\xi \quad (25)$$

Substituting (22)–(25) into the boundary condition (15), and then taking Fourier transforms about x, this leads to a set of equations which relate the spectral functions $A^{h,e}(\xi)$ to the expansion coefficients A_m^e and A_m^h as follows:

$$A^h(\xi) = \frac{k_0(\xi\widetilde{E_z} - \beta\widetilde{E_x})}{(k_0^2-\eta^2)\sin(\eta d)} \quad (26)$$

$$A^e(\xi) = \frac{jk_0^2(\xi\widetilde{E_x} + \beta\widetilde{E_z})}{\eta(k_0^2-\eta^2)\sin(\eta d)} \quad (27)$$

where

$$\widetilde{E_x} = \sum_{\nu=0}^{\infty}\left[\frac{\tau_\nu\alpha_\nu}{k_0^2}A_\nu^e - \frac{\beta}{k_0}A_\nu^h\right]j\xi U_\nu(\xi) \quad (28)$$

$$\widetilde{E_z} = \sum_{\nu=0}^{\infty}\left[\frac{\tau_\nu}{k_0}A_\nu^h + \frac{\beta\alpha_\nu}{k_0^2}A_\nu^e\right]j\tau_\nu U_\nu(\xi) \quad (29)$$

$$U_\nu(\xi) = \frac{(-1)^\nu e^{j\xi a} - e^{-j\xi a}}{\xi^2 - \tau_\nu^2}. \quad (30)$$

Substituting (21), (26) and (27) into (9) and (10) of the Hertzian vectors in region Ⅱ, then the magnetic fields $H_{x,z}^{\mathrm{II}}(x,0,z)$ derived from (26) and (27) are expressed in terms of the expansion coefficients A_m^e and A_m^h. The results are substituted into the boundary conditions (16)

for the magnetic fields together with the corresponding expressions of $H^{\mathrm{I}}_{x,z}(x,0,z)$ derived from (7) and (8). Then we integrate (16) from $x=-a$ to $x=a$ after multiplying both sides by the trigonometric functions $\sin\tau_n(x+a)$ or $\cos\tau_n(x+a)$, where n is nonnegative integers. This leads a set of linear equations for the expansion coefficients A^h_m and A^e_m as follows:

$$\begin{aligned} & a\left[\frac{\tau_n\alpha_n}{k_1k_0}A^h_n+\frac{\beta}{k_0}A^e_n\right]\cot(\alpha_n b) \\ &= \sum_{m=0}^{\infty}\left[\frac{-\tau_m\alpha_m}{k_1^2}A^e_m+\frac{\beta}{k_1}A^h_m\right]\tau_n\beta I_1(m,n) \\ &\quad -\sum_{m=0}^{\infty}\left[\frac{\beta\alpha_m}{k_1^2}A^e_m+\frac{\tau_m}{k_1}A^h_m\right]\tau_m\tau_n I_2(m,n) \\ &\qquad\qquad \text{for } n=1,2,\cdots \end{aligned} \tag{31}$$

$$\begin{aligned} & a(1+\delta_{n0})\left[\frac{-\beta\alpha_n}{k_1k_0}A^h_n+\frac{\tau_n}{k_0}A^e_n\right]\cot(\alpha_n b) \\ &= \sum_{m=0}^{\infty}\left[\frac{-\tau_m\alpha_m}{k_1^2}A^e_m+\frac{\beta}{k_1}A^h_m\right](k_0^2-\beta^2)I_1(m,n) \\ &\quad -\sum_{m=0}^{\infty}\left[\frac{\beta\alpha_m}{k_1^2}A^e_m+\frac{\tau_m}{k_1}A^h_m\right]\beta\tau_m I_1(m,n) \\ &\qquad\qquad \text{for } n=0,1,2,\cdots \end{aligned} \tag{32}$$

where

$$I_1(m,n) = \int_{-\infty}^{\infty}\frac{\xi^2U_m(\xi)U_n(-\xi)}{2\pi k_0\eta\sin(\eta d)}\left[\cos(\eta d)+\Theta\right]d\xi \tag{33}$$

$$I_2(m,n) = \int_{-\infty}^{\infty}\frac{(k_0^2-\xi^2)U_m(\xi)U_n(-\xi)}{2\pi k_0\eta\sin(\eta d)}\left[\cos(\eta d)+\Theta\right]d\xi. \tag{34}$$

We can see that the integrands of (33) and (34) become one-valued functions under introducing the modified PMB. Therefore the integrals in (33) and (34) can be evaluated by the residual calculus, and then $I_1(m,n)$ and $I_2(m,n)$ are expressed in terms of the series with very fast convergence [15]. Since these integrals are zero when $m+n$ is odd number, the system of linear equations can be decomposed into two independent sets. One corresponds the set of equations with the even number of m and n, and another one corresponds to those with the odd number of m and n. If the number of mode expansion is truncated by $m=n=N$, the set is finally rendered into a matrix equation for A^h_m and A^e_m. Then the propagation constant β can be determined from

the requirement that a nontrivial solution of the matrix equation is obtained. In order to accelerate the convergence of solutions, we take into account the singular behavior of all the components of the electric field at the metal edge. The tangential components of the electric field $\boldsymbol{E}_t$ vary as $\rho^{-1/3}$ at a 90° metallic edge and the normal component of the electric field varies as $\rho^{2/3}$ [13]. Then we expand the electric fields $E^{\mathrm{I}}_{z,x}(x,0,z)$ as follows:

$$E^{\mathrm{I}}_z(x,0,z) = \left[1-\left(\frac{x}{a}\right)^2\right]^{2/3} \sum_{l=0}^{\infty} B_l C_l^{7/6}\left(\frac{x}{a}\right) e^{-j\beta z} \tag{35}$$

$$E^{\mathrm{I}}_x(x,0,z) = \left[1-\left(\frac{x}{a}\right)^2\right]^{-1/3} \sum_{l=0}^{\infty} D_l C_l^{1/6}\left(\frac{x}{a}\right) e^{-j\beta z} \tag{36}$$

where the functions of $C_l^{7/6}\left(\frac{x}{a}\right)$ and $C_l^{1/6}\left(\frac{x}{a}\right)$ are the Gegenbauer polynomials, B_l and D_l are unknown coefficients. This method can be easily applied to another more complex edge by considering the singular behavior of the each component independently. From table of integrals [14] the integrals are found.

$$\int_0^1 \left(1-t^2\right)^{\nu-\frac{1}{2}} C^{\nu}_{2n+1}(t)\sin at dt = (-1)^n \pi \frac{\Gamma(2n+2\nu+1)J_{2n+\nu+1}(a)}{(2n+1)!\Gamma(\nu)(2a)^{\nu}} \left[\mathrm{Re}\ \nu > -\frac{1}{2},\ a>0\right] \tag{37}$$

$$\int_0^1 \left(1-t^2\right)^{\nu-\frac{1}{2}} C^{\nu}_{2n}(t)\cos at dt = (-1)^n \pi \frac{\Gamma(2n+2\nu)J_{2n+\nu}(a)}{(2n)!\Gamma(\nu)(2a)^{\nu}} \left[\mathrm{Re}\ \nu > -\frac{1}{2},\ a>0\right] \tag{38}$$

Substituting (35) and (36) into (22) and (23), respectively, and using the orthogonality of the trigonometric functions together with (37) and (38), we have

$$A^h_{\mu} = \frac{2(-1)^{[\frac{\mu}{2}]}k_1}{\tau_{\mu}^2-\beta^2} \times \begin{cases} \beta \sum\limits_{l=0,2,}^{\infty} D_l X_1(l,\mu) - j\tau_{\mu} \sum\limits_{l=1,3,}^{\infty} B_l X_2(l,\mu) & \mu \triangleq even \\ \beta \sum\limits_{l=1,3,}^{\infty} (-D_l) X_1(l,\mu) - j\tau_{\mu} \sum\limits_{l=0,2,}^{\infty} B_l X_2(l,\mu) & \mu \triangleq odd \end{cases} \tag{39}$$

$$A_\mu^e = -\frac{2(-1)^{[\frac{\mu}{2}]}k_1^2}{\alpha_\mu\left(\tau_\mu^2-\beta^2\right)} \times \begin{cases} \tau_\mu \sum\limits_{l=0,2,}^{\infty} D_l X_1(l,\mu) + j\beta \sum\limits_{l=1,3,}^{\infty} B_l X_2(l,\mu) & \mu \triangleq even \\ \tau_\mu \sum\limits_{l=1,3,}^{\infty} (-D_l) X_1(l,\mu) + j\beta \sum\limits_{l=0,2,}^{\infty} B_l X_2(l,\mu) & \mu \triangleq odd \end{cases} \tag{40}$$

where

$$X_1(l,\mu) = \frac{(-1)^{[\frac{l}{2}]}\pi\Gamma(l+\frac{1}{3})J_{l+\frac{1}{6}}(\frac{\mu\pi}{2})}{l!\Gamma(\frac{1}{6})(\mu\pi)^{\frac{1}{6}}(1+\delta_{\mu 0})} \tag{41}$$

$$X_2(l,\mu) = \frac{(-1)^{[\frac{l}{2}]}\pi\Gamma(l+\frac{7}{3})J_{l+\frac{7}{6}}(\frac{\mu\pi}{2})}{l!\Gamma(\frac{7}{6})(\mu\pi)^{\frac{7}{6}}}. \tag{42}$$

Substituting (39) and (40) for even μ into (31) and (32), a new set of linear equations in terms of the coefficients B_m and D_m is derived for the even modes as follows:

$$\begin{aligned} & -\left[\frac{j(-1)^n[k_1^2-\tau_{2n}^2]}{k_0\alpha_{2n}} \sum_{m=1}^{\infty} B_m X_2(2m\text{–}1,2n) \right. \\ & \left. + \frac{(-1)^n\tau_{2n}\beta}{k_0\alpha_{2n}} \sum_{m=0}^{\infty} D_m X_1(2m,2n)\right] a\cot(\alpha_{2n}b) \\ = & \sum_{m=0}^{\infty} D_m\tau_{2n}\beta \sum_{\nu=0}^{\infty}(-1)^\nu X_1(2m,2\nu) I_1(2m,2n) \\ & + j\sum_{m=1}^{\infty} B_m\tau_{2n} \sum_{\nu=1}^{\infty}(-1)^\nu X_2(2m\text{–}1,2\nu)\tau_{2\nu} I_2(2m,2n) \\ & \qquad\qquad \text{for } n=1,2,\cdots \end{aligned} \tag{43}$$

$$\begin{aligned} & \left[-j\frac{(-1)^n[k_1^2-\beta^2]}{k_0\alpha_{2n}} \sum_{m=0}^{\infty} D_m X_1(2m,2n) \right. \\ & \left. + \frac{(-1)^n\beta\tau_{2n}}{k_0\alpha_{2n}} \sum_{m=1}^{\infty} B_m X_2(2m\text{–}1,2n)\right] a(1+\delta_{n0})\cot(\alpha_{2n}b) \\ = & \; j\sum_{m=0}^{\infty}(k_0^2-\beta^2) D_m \sum_{\nu=0}^{\infty}(-1)^\nu X_1(2m,2\nu) I_1(2m,2n) \end{aligned}$$

$$- \sum_{m=1}^{\infty} \beta B_m \sum_{\nu=1}^{\infty} (-1)^{\nu} \tau_{2\nu} X_2(2m\text{–}1, 2\nu) I_1(2m, 2n)$$

$$\text{for } n = 0, 1, 2, \cdots \tag{44}$$

When the number of expansion coefficients is truncated by $m = n = N$, the linear system (39) and (40) is finally rendered into a matrix equation for B_m and D_m. Then the propagation constant β of even modes can be determined from the requirement that a nontrivial solution of the matrix equation is obtained. In the same way, the matrix equation for the odd modes is derived by substituting (39) and (40) for odd μ to (31) and (32).

Table 1. Convergence of the normalized propagation constant β/k_0 of the dominant mode of an inset dielectric guide as the function of location c/λ of assuming PEC and PMC boundaries with different width d/λ of the buffer region.

d/λ	c/λ	0.3	0.5	0.7	1.0	2.0
0.05	Re(β/k_0)	1.20764267	1.20805813	1.20806855	1.20806848	1.20806660
	Im(β/k_0)	-0.0001312	-0.0001307	-0.0001306	-0.0001306	-0.0001306
0.15	Re(β/k_0)	1.20696546	1.20804213	1.20806817	1.20806855	1.20806672
	Im(β/k_0)	-0.0001318	-0.0001307	-0.0001306	-0.0001306	-0.0001306
Frequency=8GHz, 2a=10.16 mm, b=15.24 mm, ϵ_r=(2.08 -j0.000416) N=2						

4. NUMERICAL RESULTS

The proposed method has been applied to the analysis of an inset dielectric guide with a single-layered or double-layered dielectric. We first consider the single-layered inset dielectric guide. The convergence of the normalized propagation constant β/k_0 of the fundamental mode is shown in Table 1 as the function of location of assumed PEC and PMC boundaries with different width of the buffer region for $2a = 10.16\,\text{mm}$, $b = 15.24\,\text{mm}$, $\epsilon_r = 2.08 - j0.000416$, and $f = 8\,\text{GHz}$. The truncation number of mode expansion is chosen to be $N = 2$. It is seen that the relative errors in the propagation constant are less than 0.0002% when the width d/λ of buffer region and the location c/λ of PEC and PMC boundaries are greater than 0.05 and 0.7, respectively. From this results the virtual boundary may be regarded as a perfectly matched boundary. The propagation constants β of the fundamental mode for various frequencies are shown in Table 2 as the function of the mode truncation number N and compared with those obtained by the TRD method [2] and the measured data [8]. The buffer width and the location of the PEC (or PMC) boundary is assumed at $d/\lambda = 0.05$ and

Table 2. Convergence of the propagation constant β (m^{-1}) as the function of mode truncation number N, where $d/\lambda = 0.05$, $c/\lambda = 0.75$ and the values of other parameters are the same as those given in Table 1.

f (GHz)		Present Method					TRD Ref.[2]		Meas.
		N=0	N=1	N=2	N=3	N=4	(M=1)	(M=3)	Ref.[8]
7	Re(β)	170.8203	170.9221	170.9394	170.9448	170.9470	171.43	170.95	170.056
	Im(β)	-0.01845	-0.01838	-0.01838	-0.01838	-0.01838	-0.0185	-0.0183	
8	Re(β)	202.4725	202.5331	202.5487	202.5538	202.5560	203.07	202.57	202.008
	Im(β)	-0.02200	-0.02191	-0.02190	-0.02190	-0.02190	-0.0220	-0.0219	
9	Re(β)	234.0830	234.1036	234.1171	234.1218	234.1239	234.64	234.13	232.297
	Im(β)	-0.02550	-0.02541	-0.02540	-0.02540	-0.02540	-0.0255	-0.0254	
10	Re(β)	265.6665	265.6511	265.6624	265.6667	265.6686	266.17	265.68	264.138
	Im(β)	-0.02896	-0.02887	-0.02887	-0.02886	-0.02886	-0.0289	-0.0289	
11	Re(β)	297.2214	297.1757	297.1849	297.1887	297.1904	297.68	297.20	293.914
	Im(β)	-0.03238	-0.03229	-0.03229	-0.03228	-0.03228	-0.0323	-0.0323	
12	Re(β)	328.7404	328.6703	328.6775	328.6809	328.6824	329.14	328.69	325.806
	Im(β)	-0.03574	-0.03567	-0.03566	-0.03566	-0.03566	-0.0357	-0.0356	
13	Re(β)	360.2155	360.1267	360.1321	360.1351	360.1365	360.57	360.15	357.388
	Im(β)	-0.03906	-0.03899	-0.03898	-0.03898	-0.03898	-0.0390	-0.0390	

$c/\lambda = 0.75$, respectively, and the values of other parameters are the same as those given in Table 1. The results of the present method are in very good agreement with those of TRD method and the measured data. It is note that the relative errors by the present method are less than 0.07% even if only one expansion coefficient with $N = 0$ is considered.

Figure 2 shows the convergence of the propagation constant of dominant mode as functions of the location c/λ of PEC and PMC boundaries. The curves $\boldsymbol{a}$, $\boldsymbol{b}$ and $\boldsymbol{c}$ were obtained by the present perfectly matched boundary with the buffer width $d/\lambda = 0.05,\ 0.15,\ 0.25$. The curves $\boldsymbol{d}$ and $\boldsymbol{e}$ were obtained by PEC boundary and PMC boundary, respectively, without the buffer region. We can see that the convergence is much faster in the perfectly matched boundary than in the PEC or PMC boundary. It is worth emphasizing that the calculation of the integrals of (33) and (34) becomes easier as the value d/λ decreases. This results confirm the effectiveness of the perfectly matched boundary.

Table 3 shows the convergence of the propagation constant β of the dominant mode of an inset dielectric guide for different widths d/λ of the buffer region. When the buffer width is zero, the propagation

Table 3. Convergence of the propagation constant β (m^{-1}) of the dominant mode of an inset dielectric guide for different widths d/λ of the buffer region. The values of other parameters are the same as those given in Table 1.

d/λ		$N=0$	$N=1$	$N=2$	$N=3$	$N=4$
0	Re(β)	217.871466	217.871440	217.871439	217.871439	217.871439
	Im(β)	-0.02359913	-0.02359917	-0.02359917	-0.02359917	-0.02359917
0.05	Re(β)	218.281513	218.3217184	218.336326	218.341254	218.343365
	Im(β)	-0.02374682	-0.02366141	-0.02365620	-0.02365503	-0.02365459
f=8.5 GHz, $c/\lambda = 0.75$						

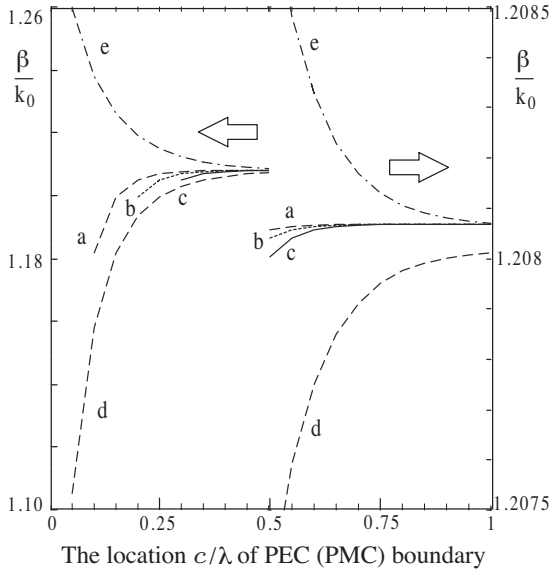

Figure 2. Convergence of the propagation constant of dominant mode as functions of the location c/λ of virtual boundaries. The curves ***a***, ***b*** and ***c*** are obtained by the present matched boundary with the buffer width $d/\lambda = 0.05,\ 0.15$ and 0.25, respectively. The curves ***d*** and ***e*** are obtained by PEC boundary and PMC boundary, respectively, without buffer region.

constant does not change with the increase of mode truncation number N. When the buffer region $d/\lambda = 0.05$ is introduced, on the other hand, the propagation constant converges appropriately as the mode truncation number increases. This comparison demonstrates that the insertion of finite buffer region is very important in the analysis of an

Table 4. Convergence of the propagation constant β (m^{-1}) calculated from the different linear systems, where $d/\lambda = 0.05$, $c/\lambda = 0.75$, $f = 8.5\,\mathrm{GHz}$, and the values of other parameters are the same as those given in Table 1.

Eqs. (43) and (44)					
	$N=0$	$N=1$	$N=2$	$N=3$	$N=4$
$\mathrm{Re}(\beta)$	218.281513	218.3217184	218.336326	218.341254	218.343365
$\mathrm{Im}(\beta)$	-0.02374682	-0.02366141	-0.02365620	-0.02365503	-0.02365459
Eqs. (31) and (32)					
	$N=0$	$N=10$	$N=20$	$N=30$	$N=40$
$\mathrm{Re}(\beta)$	217.871550	218.3049011	218.327717	218.334994	218.338435
$\mathrm{Im}(\beta)$	-0.02359921	-0.02364815	-0.02365146	-0.02365248	-0.02365296

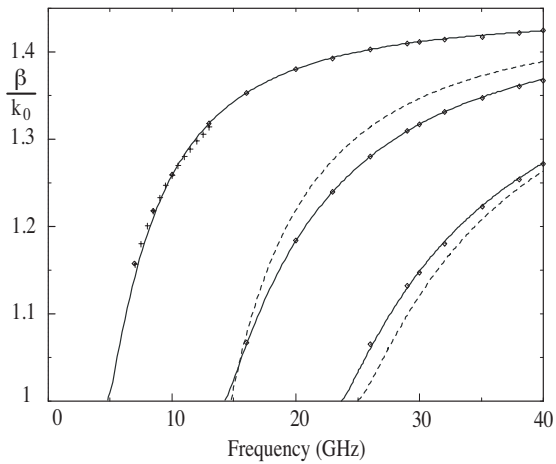

Figure 3. The normalized propagation constants β/k_0 of several lowest modes for a single-layered dielectric guide obtained for $c/\lambda = 0.7$, $d/\lambda = 0.05$ and $N = 0$. The lines are the results by the present method, the solid lines indicate the even modes, and the dash lines indicate the odd modes. The diamond symbols are the results by TRD approach [2], and the cross symbols are the measured data [8].

inset guide using the perfectly matched boundary. Table 4 shows the convergence of the propagation constant β calculated from the different linear systems. It is seen that the convergence behavior is noticeably improved by introducing the edge condition into the expansion of the aperture fields (35) and (36).

Figure 3 shows the dispersion curves of several lowest even modes

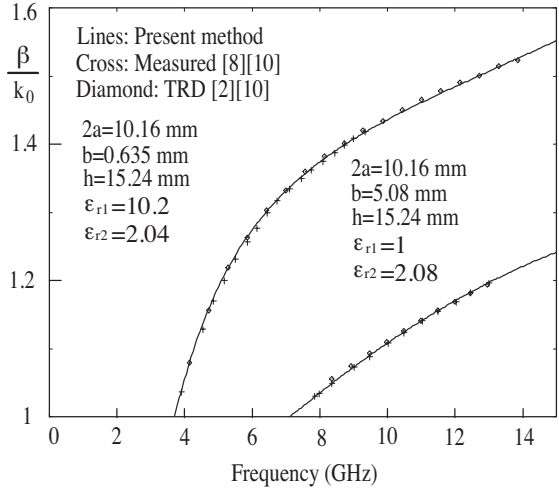

Figure 4a. The normalized propagation constants β/k_0 of several lowest modes for a single-layered dielectric guide obtained for $c/\lambda = 0.7$, $d/\lambda = 0.05$ and $N = 0$.

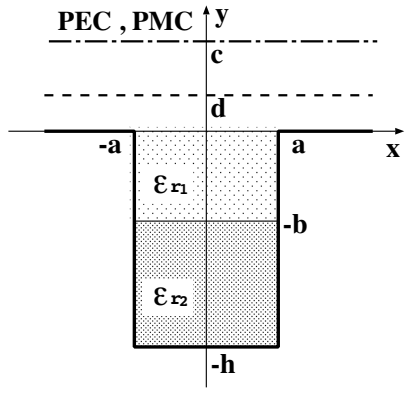

Figure 4b. Cross section of a double-layered inset dielectric guide.

and odd modes in x-band for the single-layered inset dielectric guide with the same configuration parameters given in Table 1. The PEC and PMC boundaries are assumed at $c/\lambda = 0.7$, the buffer width is $d/\lambda = 0.05$, and only one expansion coefficient with $N = 0$ is considered on the aperture. The present results are in close agreement with those of TRD method [2] and the measured data [8]. Figure 4(a) shows the dispersion curves of the fundamental mode of two double-

layered inset dielectric guides, whose geometry is shown in Figure 4(b), with $c/\lambda = 0.7$, $d/\lambda = 0.5$ and $N = 0$. We can see again that the present results are in close agreement with those of literatures [2, 8, 10].

5. CONCLUSION

A fast and efficient method for the analysis of inset dielectric guides has been presented using the Fourier transform technique with a modified perfectly matched boundary. In this approach, a novel idea, modified perfectly matched boundary, has been proposed in order to deal with the open region. This modified PMB avoids the numerical integral, then the accuracy of the numerical solution has been improved and the computer time has been reduced. Moreover, the singular behavior of the fields at metal edge is taken into account in the analysis. It is shown that the convergence of the solution is very fast and relative error less than 0.07% is attained even if only the first term is considered in the field expansion of the guide. The numerical result of the propagation constants for single- and double-layered inset dielectric guide agree well with those of literatures.

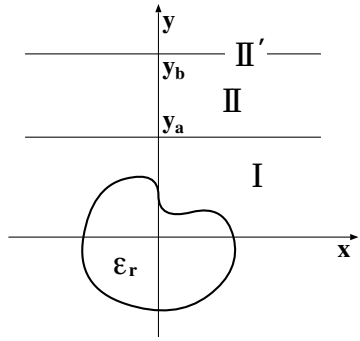

Figure 5. Cross section of a waveguide.

APPENDIX A. PROOF OF THE MODIFIED PMB CONDITION

The cross section of an open-waveguide is shown in Figure 5, where PEC (or PMC) located at the plane $y = y_b$ is a virtual boundary. The cross sectional area is divided into two regions I and II′. The region II′ denotes the upper semi-infinite ($y > y_a$) free-space of the original guide without PEC and PMC boundaries, and the region II denotes the free-space within $y_a \leq y \leq y_b$ bounded by the virtual PEC and

PMC boundaries. The original fields in the region II' can be expressed by the electric and magnetic Hertzian vectors as follows:

$$\mathbf{\Pi}^e(x,y,z) = \frac{\hat{y}}{2\pi}\int_{-\infty}^{\infty} A^e(\xi)e^{-j(\xi x+\eta y+\beta z)}d\xi \quad \text{(A1)}$$

$$\mathbf{\Pi}^h(x,y,z) = \frac{\hat{y}}{2\pi}\int_{-\infty}^{\infty} A^h(\xi)e^{-j(\xi x+\eta y+\beta z)}d\xi \quad \text{(A2)}$$

where $\eta = \sqrt{k_0^2-\xi^2-\beta^2}$, $k_0 = \omega\sqrt{\mu_0\epsilon_0}$ is the wave number and β is the propagation constant of a waveguide mode. The spectral functions $A^h(\xi)$ and $A^e(\xi)$ can be expressed by the tangential components of the electric fields on the plane of $y = y_a$.

$$A^e(\xi) = -\frac{e^{j(\eta y_a+\beta z)}}{\eta(\xi^2+\beta^2)}\left[\xi\widetilde{E_x}(x,y_a,z)+\beta\widetilde{E_z}(x,y_a,z)\right] \quad \text{(A3)}$$

$$A^h(\xi) = \frac{e^{j(\eta y_a+\beta z)}}{k_0 Z_0(\xi^2+\beta^2)}\left[\beta\widetilde{E_x}(x,y_a,z)-\xi\widetilde{E_z}(x,y_a,z)\right] \quad \text{(A4)}$$

where

$$\widetilde{E} = \int_{-\infty}^{\infty} Ee^{j\xi x}dx \quad \text{(A5)}$$

and $Z_0 = \sqrt{\mu_0/\epsilon_0}$ is the intrinsic impedance in free space. Substituting (A3) and (A4) into (A1) and (A2), we have

$$\mathbf{\Pi}^e(x,y,z) = \frac{\hat{y}}{2\pi}\int_{-\infty}^{\infty} -\frac{e^{j\eta(y_a-y)}}{\eta(\xi^2+\beta^2)}\left[\xi\widetilde{E_x}(x,y_a,z)+\beta\widetilde{E_z}(x,y_a,z)\right]e^{-j\xi x}d\xi \quad \text{(A6)}$$

$$\mathbf{\Pi}^h(x,y,z) = \frac{\hat{y}}{2\pi}\int_{-\infty}^{\infty} \frac{e^{j\eta(y_a-y)}}{k_0 Z_0(\xi^2+\beta^2)}\left[\beta\widetilde{E_x}(x,y_a,z)-\xi\widetilde{E_z}(x,y_a,z)\right]e^{-j\xi x}d\xi \quad \text{(A7)}$$

From (A6) and (A7), the tangential components of magnetic fields can be derived as follows:

$$H_x(x,y_a,z) = \int_{-\infty}^{\infty} e^{-j\xi x}\frac{\beta\xi\widetilde{E_x}(x,y_a,z)+(k_0^2-\xi^2)\widetilde{E_z}(x,y_a,z)}{2\pi Z_0 k_0\eta}d\xi \quad \text{(A8)}$$

$$H_z(x,y_a,z) = -\int_{-\infty}^{\infty} e^{-j\xi x}\frac{(k_0^2-\beta^2)\widetilde{E_x}(x,y_a,z)+\beta\xi\widetilde{E_z}(x,y_a,z)}{2\pi Z_0 k_0\eta}d\xi \quad \text{(A9)}$$

Up to now, we have obtained the exact expression of the tangential components of magnetic fields on the boundary plane $y = y_a$ for the original problem.

In the same way, the fields in the region Ⅱ with PEC located at the plane $y = y_b$ can be expressed by the Hertzian vectors, which can be written in terms of the tangential components of electric fields $[E_{xe}(x, y_a, z), E_{ze}(x, y_a, z)]$ on the plane $y = y_a$.

$$\begin{aligned}\mathbf{\Pi}_e^e(x,y,z) &= \frac{\hat{y}}{2\pi}\int_{-\infty}^{\infty}\frac{-j}{\eta(\xi^2+\beta^2)}\frac{\cos\eta(y-y_b)}{\sin\eta(y_a-y_b)} \\ &\quad\times\left[\xi\widetilde{E_{xe}}(x,y_a,z)+\beta\widetilde{E_{ze}}(x,y_a,z)\right]e^{-j\xi x}d\xi \quad \text{(A10)}\\ \mathbf{\Pi}_e^h(x,y,z) &= \frac{\hat{y}}{2\pi}\int_{-\infty}^{\infty}\frac{\sin\eta(y-y_b)}{k_0Z_0(\xi^2+\beta^2)\sin\eta(y_a-y_b)} \\ &\quad\times\left[\beta\widetilde{E_{xe}}(x,y_a,z)-\xi\widetilde{E_{ze}}(x,y_a,z)\right]e^{-j\xi x}d\xi \quad \text{(A11)}\end{aligned}$$

The tangential components of magnetic fields on the boundary plane $y = y_a$ can be derived from (A10) and (A11).

$$\begin{aligned}H_{xe}(x,y_a,z) &= \int_{-\infty}^{\infty}e^{-j\xi x}j\cot\eta(y_a-y_b) \\ &\quad\times\frac{\beta\xi\widetilde{E_{xe}}(x,y_a,z)+(k_0^2-\xi^2)\xi\widetilde{E_{ze}}(x,y_a,z)}{2\pi Z_0k_0\eta}d\xi \quad \text{(A12)}\\ H_{ze}(x,y_a,z) &= -\int_{-\infty}^{\infty}e^{-j\xi x}j\cot\eta(y_a-y_b) \\ &\quad\times\frac{(k_0^2-\beta^2)\widetilde{E_{xe}}(x,y_a,z)+\beta\xi\widetilde{E_{ze}}(x,y_a,z)}{2\pi Z_0k_0\eta}d\xi \quad \text{(A13)}\end{aligned}$$

If assume $|\beta| > k_0$ and $E_{xe,ze}(x, y_a, z) = E_{x,z}(x, y_a, z)$, by comparing (A8) and (A9) with (A12) and (A13), respectively. Since

$$j\cot\eta(y_a-y_b)=\frac{1}{1-\alpha}\overset{|\alpha|<1}{\Longleftrightarrow}1+\alpha+O(\alpha^2), \quad \text{(A14)}$$

we have

$$H_{xe,ze}(x,y_a,z)=H_{x,z}(x,y_a,z)+O(\alpha) \quad \text{(A15)}$$

where

$$\alpha=\frac{2e^{j2\eta(y_a-y_b)}}{1+e^{j2\eta(y_a-y_b)}}. \quad \text{(A16)}$$

When $|\beta| > k_0$, we have Im $(\eta) < 0$, for $\forall\xi \in$ R and $|\alpha| < 1$, $\lim_{y_b-y_a\to\infty}\alpha = 0$. From uniqueness theorem, we conclude that the fields in the region I with the virtual PEC boundary differs from those

of the original problem without PEC, and the difference is dependent on α. The reason is that the boundary values on the plane $y = y_a$ with PEC approximate to the original boundary values without PEC, as shown in (A15), and the errors of the approximate values are in proportion to α. For PMC case, we have

$$\begin{aligned}
\mathbf{\Pi}_m^e(x,y,z) &= \frac{\hat{y}}{2\pi}\int_{-\infty}^{\infty}\frac{j}{\eta(\xi^2+\beta^2)}\frac{\sin\eta(y-y_b)}{\cos\eta(y_a-y_b)} \\
&\quad\times\left[\xi\widetilde{E_{xm}}(x,y_a,z)+\beta\widetilde{E_{zm}}(x,y_a,z)\right]e^{-j\xi x}d\xi \qquad \text{(A17)} \\
\mathbf{\Pi}_m^h(x,y,z) &= \frac{\hat{y}}{2\pi}\int_{-\infty}^{\infty}\frac{\cos\eta(y-y_b)}{k_0Z_0(\xi^2+\beta^2)\cos\eta(y_a-y_b)} \\
&\quad\times\left[\beta\widetilde{E_{xm}}(x,y_a,z)-\xi\widetilde{E_{zm}}(x,y_a,z)\right]e^{-j\xi x}d\xi \qquad \text{(A18)} \\
H_{xm}(x,y_a,z) &= -\int_{-\infty}^{\infty}e^{-j\xi x}j\tan\eta(y_a-y_b) \\
&\quad\times\frac{\beta\xi\widetilde{E_{xm}}(x,y_a,z)+(k_0^2-\xi^2)\widetilde{E_{zm}}(x,y_a,z)}{2\pi Z_0k_0\eta}d\xi \qquad \text{(A19)} \\
H_{zm}(x,y_a,z) &= \int_{-\infty}^{\infty}e^{-j\xi x}j\tan\eta(y_a-y_b) \\
&\quad\times\frac{(k_0^2-\beta^2)\widetilde{E_{xm}}(x,y_a,z)+\beta\xi\widetilde{E_{zm}}(x,y_a,z)}{2\pi Z_0k_0\eta}d\xi \qquad \text{(A20)}
\end{aligned}$$

Assuming $|\beta| > k_0$, $E_{xm,zm}(x,y_a,z) = E_{x,z}(x,y_a,z)$, and comparing (A8) and (A9) with (A19) and (A20), respectively, we obtain the same conclusion with the PEC case. On the other hand, if assuming $E_{xe,ze}(x,y_a,z) = E_{xm,zm}(x,y_a,z) = E_{x,z}(x,y_a,z)$, which corresponds to (1) and (3), and considering

$$\begin{aligned}
&\frac{1}{2}\left[j\cot\eta(y_a-y_b)-j\tan\eta(y_a-y_b)\right] \\
&=\frac{1}{2}\left[\frac{1}{1-\alpha}+1-\alpha\right]\overset{|\alpha|<1}{\Longleftrightarrow}1+\frac{\alpha^2}{2}+O(\alpha^3), \qquad \text{(A21)}
\end{aligned}$$

we have

$$\begin{aligned}
&\frac{H_{xe,ze}(x,y_a,z)+H_{xm,zm}(x,y_a,z)}{2} \\
&= H_{x,z}(x,y_a,z)+O(\alpha^2/2). \qquad \text{(A22)}
\end{aligned}$$

Comparing (A22) with (A15), we can see that the values of the tangential components of magnetic fields is much closer to those of

the original structure by the modified PMB than by only PEC and by only PMC. This means that the accuracy of the obtained solution is much higher with the modified PMB, whose boundary conditions are the continuous conditions (1) and (2) with the additional constraints (3), than with the only PEC (and with only PMC). For the rest three choices of the additional constraints, the same conclusions can be proved too in the same way.

REFERENCES

1. Itoh, T. and B. Adelseck, "Trapped image guide for millimeter-wave circuits," *IEEE Trans. Microwave Theory Tech.,* Vol. MTT-28, No. 12, 1433–1436, Dec. 1980.
2. Rozzi, T. and S. J. Hedges, "Rigorous analysis and network modeling of the inset dielectric guide," *IEEE Trans. Microwave Theory Tech.,* Vol. MTT-35, No. 9, 823–834, Sept. 1987.
3. Hedes, S. and T. Rozzi, "The loss analysis of inset dielectric guide including bending loss and a comparison with image line," *Proc. 17th European Microwave Conf.,* 933–938, 1987.
4. Ma, L., S. R. Pennock, and T. Rozzi, "Linear arrays realized in IDG," *IEE Coloquium Components for Novel Transmission Lines,* Dig. No. 1990/048, London, March 26, 1990.
5. Gelsthorpe, R. V., *et al.*, "Dielectric waveguide: A low-cost technology for millimeter wave integrated circuits," *Radio Electron. Eng.,* Vol. 52. Nos. 11/12, 552–528, Nov./Dec. 1982.
6. Rozzi, T. and L. Ma, "Mode compleleteness, normalization and Green's function of the inset dielectric guide," *IEEE Trans. Microwave Theory Tech.,* Vol. MTT-36, No. 3, 542–551, Mar. 1988.
7. Zhou, W. and T. Itoh, "Analysis of trapped image guide using effective dielectric constant and surface impedances," *IEEE Trans. Microwave Theory Tech.,* Vol. MTT-30, No. 12, 2163–2166, Dec. 1982.
8. Rozzi, T., S. R. Pennock, and D. Boscovic, "Dispersion characteristics of coupled inset dielectric guides," *Proc. 20th European Microwave Conf.,* 1175–1180, 1990.
9. Pennock, S. R., D. M. Boškovià, and T. Rozzi, "Analysis of coupled inset dielectric guide under LSE and LSM polarization," *IEEE Trans. Microwave Theory Tech.,* Vol. MTT-40, No. 5, 916–924, May 1992.
10. Pennock, S. R., N. Izzat, and T. Rozzi, "Very wideband operation

of twin-layer inset dielectric guide," *IEEE Trans. Microwave Theory Tech.,* Vol. MTT-40, No. 10, 1910–1917, Oct. 1992.

11. Ma, Z. and E. Yamashita, "Accurate analysis of inset dielectric guide structures using an efficient mode-matching method," *Proc. 6th Int. Symp. on RAMT.,* 102–105, 1997.
12. Shen, Z. and R. H. Macphie, "Modeling of a monopole partially buried in a grounded dielectric substrate by the modal expansion method," *IEEE Trans. Antennas Propagat.,* Vol. AP-44, 1535–1536, Nov. 1996.
13. Mittra, R. and S. W. Lee, *Analytical Techniques in the Theory of Guided Waves,* Macmillan, New York.
14. Gradshteyn, I. S. and I. M. Ryshik, *Table of Integrals, Series and Products,* Academic Press, New York, 1965.
15. Jia, H., K. Yoshitomi, and K. Yasumoto, "Rigorous analysis of rectangular waveguide junctions by Fourier transform technique," *Progress In Electromagnetics Research,* PIER 20, 261–280, 1998.